FAST PHOTOTHERMAL INSPECTION OF PLASMA-SPRAYED COATINGS OF PRIMARY CIRCULATION SEAL RINGS OF A NUCLEAR REACTOR. PART TWO: AFTER THE TRIAL RUN

R. Lehtiniemi, J. Hartikainen, J. Rantala, J. Varis, and M. Luukkala
University of Helsinki, Department of Physics
Siltavuorenpenger 20 D, SF-00170 Helsinki, Finland

INTRODUCTION

In the 1991 QNDE conference [1] we described a photothermal inspection of the plasma-sprayed coatings of two seal rings used in the main pump of the primary circulation in the PWR-type nuclear reactor. The measurements concentrated on detecting the most critical flaw type, adhesion defects at the interface between the coating and the substrate. The samples were tested immediately after they were coated and lapped, and already then two thermal anomalies could be found.

Afterwards, the samples were subjected to a 1,600 hours trial run and inspected again with the same method. The results of this second inspection round are presented here.

THE SAMPLE AND THE MEASUREMENT SYSTEM

The sample is a pair (a rotor and a stator) of seal rings made of stainless steel and coated with 300 μm thick plasma-sprayed chromium oxide layer in order to increase the resistance to mechanical strain. The outer diameter of the ring is approximately 27 cm and the width of the coated area to be inspected is 3.7 cm.

The inspection is based on laser heating. The beam is focussed on a line on the coated surface of the sample (Fig. 1). The temperature rise of the coating is monitored with an infrared line scanner, the imaging line of which is parallel to the laser line. A thermal image is constructed by rotating the sample perpendicularly to the heating and scanning lines, when the area imaged with a single measurement is about 10 cm x 1,5 cm. The system is described in more detail in Ref. [1].

Review of Progress in Quantitative Nondestructive Evaluation, Vol. 12
Edited by D.O. Thompson and D.E. Chimenti, Plenum Press, New York, 1993

The coatings of both rings were inspected in 79 partially overlapping measurements (including double-checks) producing as many thermal images. The measurement time was 65 seconds per image.

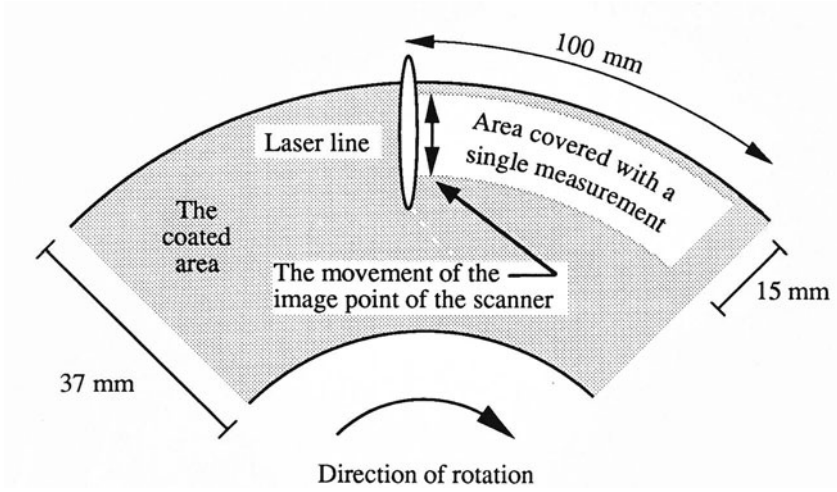

Fig. 1. The arrangement of measurement.

As an example of the measurements, in Figs 2 and 3 a visual microscopic and a thermal image of the same part of the coating are shown. In the visual image, a few areas of surface damages appeared during the trial run are visible near the inner edge of the coating. These damages can be seen also in the thermal area as cooler (darker) areas because of the different absorption and emission characteristics of the damaged parts. However, the actual adhesion defect appearing warmer (brighter, pointed with the cursor arrow) in the thermal image cannot be detected in the visual image. The horizontal stripes in the thermal images are artifacts caused by the digital image enhancement technique used for correcting the effect of the Gaussian heating profile. The dark, vertical stripe below the defect is due to the AC-coupling of the IR detector.

A pair of visual and thermal images is shown also in Figs 4 and 5. In the visual image a narrow ridge and a polished zone (arrow) caused by the trial run are clearly seen. Instead, two adhesion defects appearing in the thermal image cannot be visually detected.

Figs 6 and 7 present a couple of typical measurement results of the areas with adhesion defects. In Fig. 6 two defects are well detectable as warmer areas. In the image also a darker oval-shaped area of higher thermal diffusivity appeared during the trial run can be seen. A few anomalies of this kind could be detected but, however, they do not indicate adhesion defects. In Fig. 7, a common type of the defects found is shown. The warmer defect is surrounded by a cooler area of higher diffusivity. Also a edge worn out into the coating (see Fig. 4) stands out as a warmer area because of its different geometry.

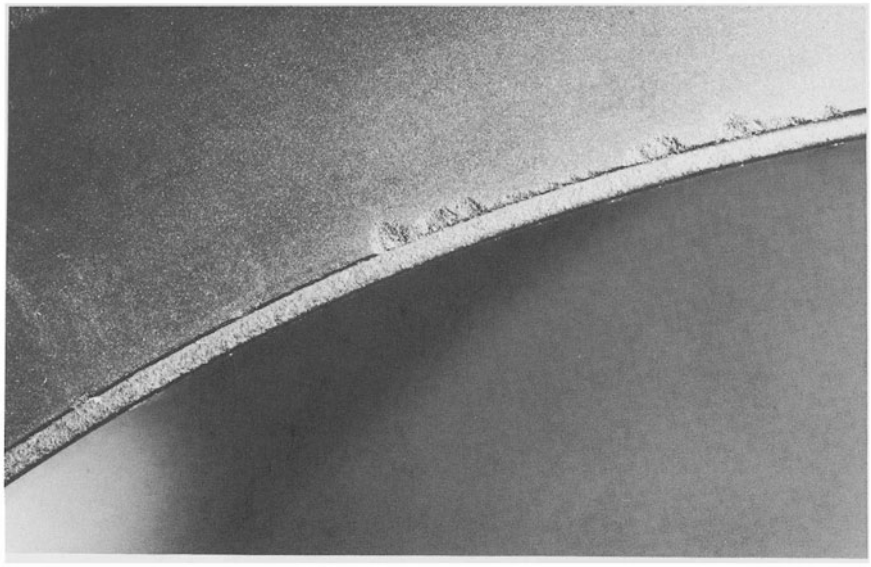

Fig. 2. A microscopic visual image of the coating. A few surface defects are clearly seen.

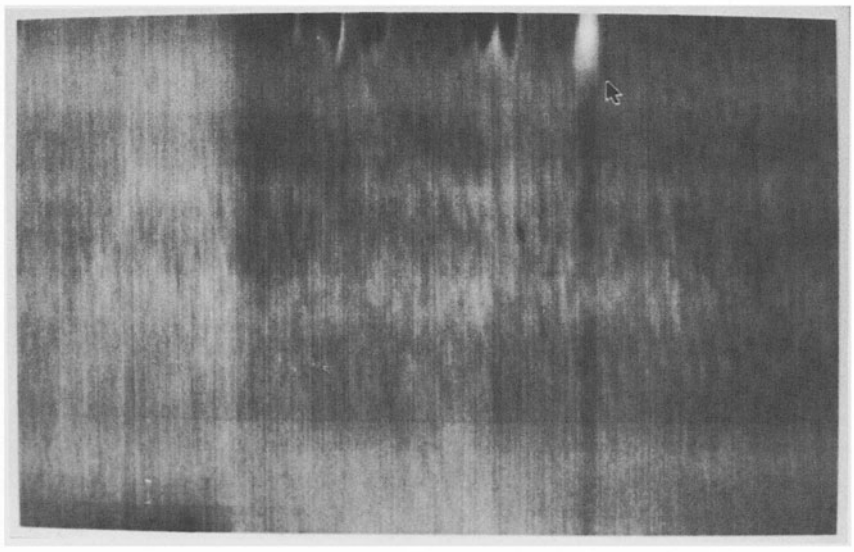

Fig. 3. A thermal image of the coating of the same area as in the Fig. 2. In addition to the surface defects, also an actual adhesion defect that is not detectable in the visual image appears as a brighter area pointed by an arrow.

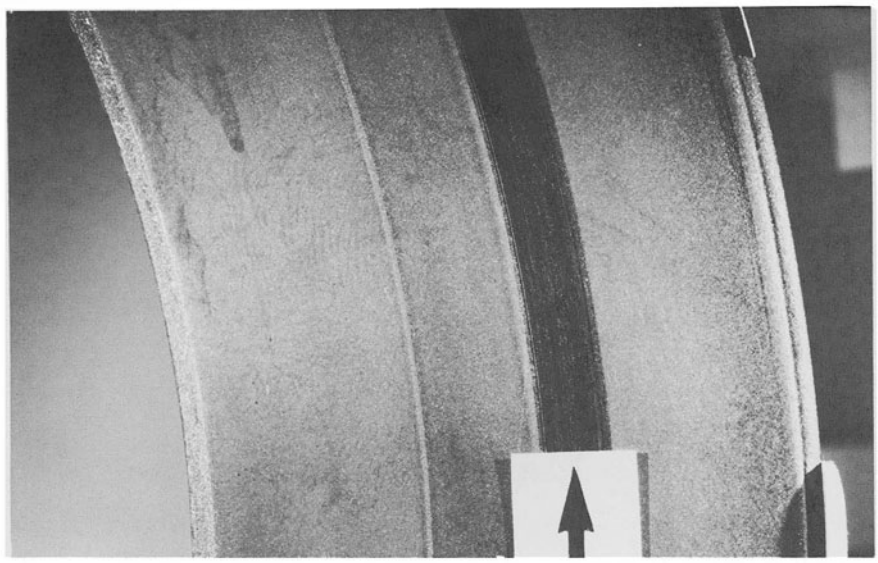

Fig. 4. A microscopic visual image of the coating with surface structure caused by the trial run.

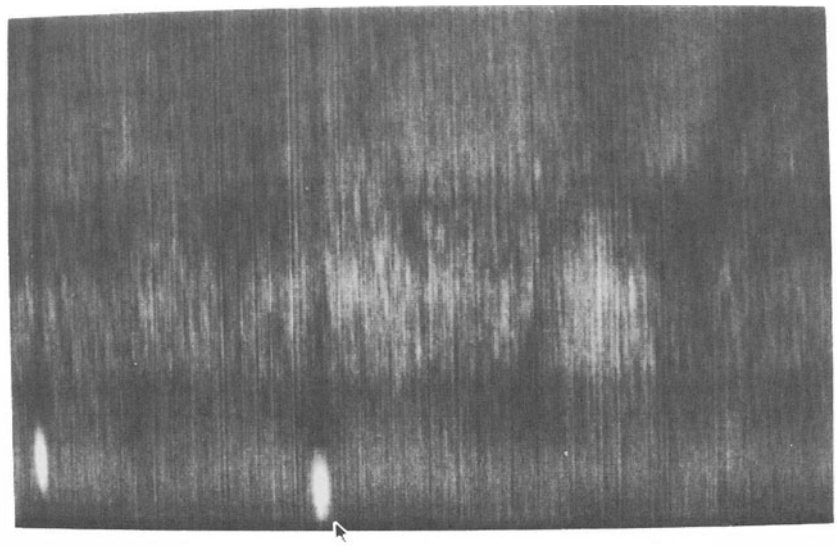

Fig. 5. A thermal image of the coating of the same area as in the Fig. 4. Two adhesion defects which are not detectable in the visual image appear as brighter areas.

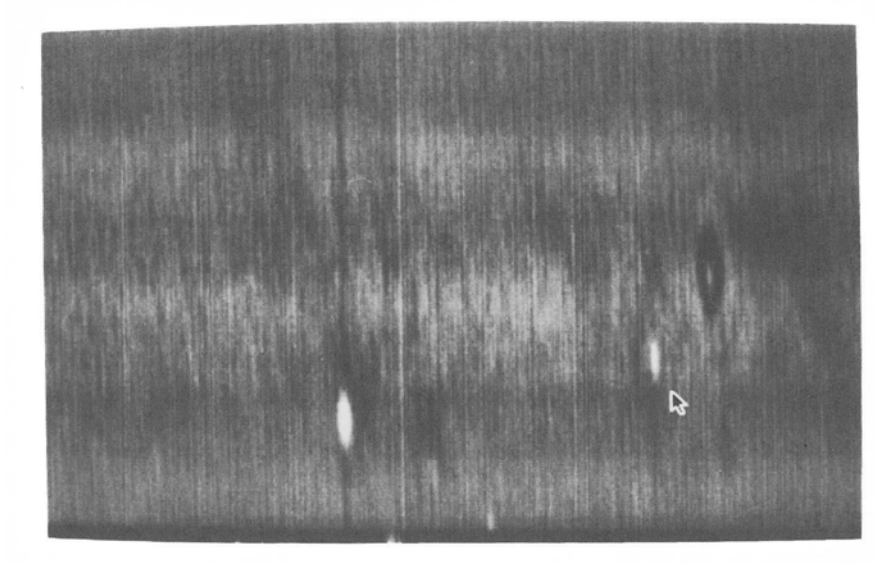

Fig. 6. A thermal image of two adhesion defects which are not detectable in the visual image, but distinguish clearly in the thermal image as brighter areas.

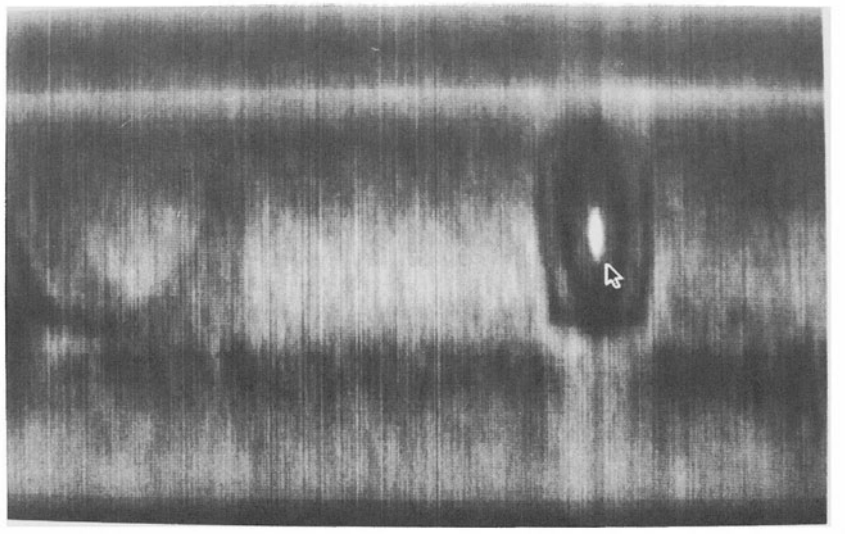

Fig. 7. A thermal image of a defect surrounded by a cooler area of higher diffusivity.

The locations of the detected defects are shown in Figs 8 a) and b). In Fig. 8 a), the defects found from the rotor ring are discerned as white areas. Also the two defects detected before the trial run and some dimensions of the sample are marked in the picture. In Fig. 8 b), the defects in the stator ring are shown. The defects surrounded by areas of higher thermal diffusivity are shown as dark circles.

As can be seen, several defects are physically situated near the edges of the coatings which are quite probable sites for adhesion failures. Typical dimensions of the defects are below 2 mm x 2 mm. The defects in the stator ring are concentrated in certain areas, which may have been under the greatest exertion. About one half of these flaws are surrounded by areas of higher diffusivities. An interesting result is that the defects found already in the first inspection round before the trial run did not grow or become more serious during the trial run. Also, the stator ring seems to have been under greater stress judging by the much larger number of the defects arisen during the trial run.

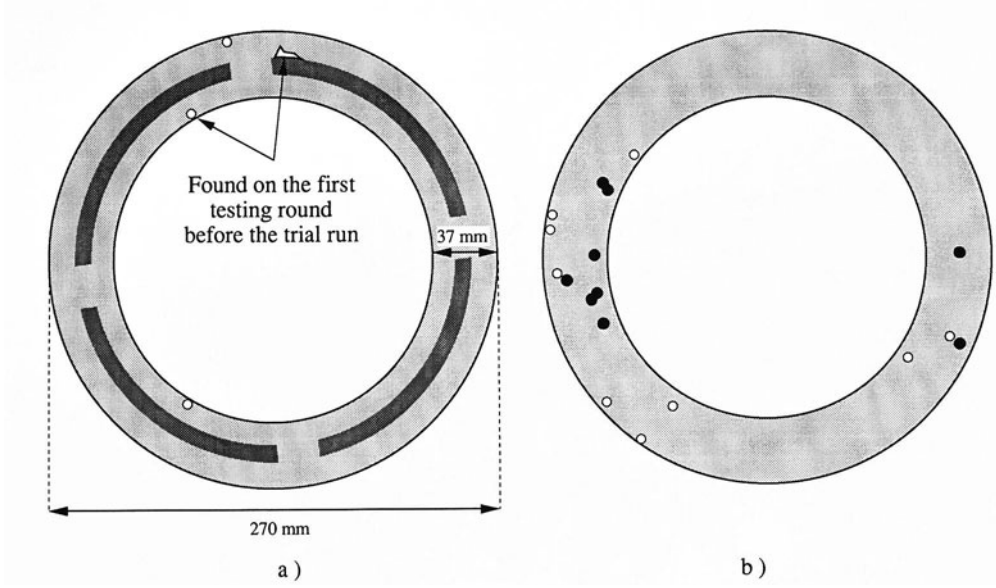

Fig. 8. A schematic drawing about the locations of the adhesion defects found a) from the rotor ring and b) from the stator ring. Defects surrounded by areas of higher diffusivity are shown as dark circles.

CONCLUSIONS

The appearance of the numerous delamination defects during the trial run simulating the real environment of use emphasizes the importance of a reliable NDE method for this purpose. The effectiveness of the photothermal method applied to this practical problem of major importance has been quite clearly demonstrated in this study, which has already lead to practical applications.

ACKNOWLEDGEMENTS

The authors would like to thank Imatran Voima OY for fruitful collaboration and Mr. Pekka Pihkala for technical assistance. A financial support from the Foundation of Jenny and Antti Wihuri is gratefully acknowledged.

REFERENCES

1. R. Lehtiniemi, J. Hartikainen, J. Rantala, J. Varis, and M. Luukkala, in *Review of Progress in Quantitative NDE*, Vol. 11 A, edited by D. O.Thompson and D. E. Chimenti (Plenum Press, New York, 1991), p. 441.